

Properties of porous $\text{FeAlO}_y/\text{FeAl}_x$ ceramic matrix composite influenced by mechanical activation of FeAl powder

V USOLTSEV¹, S TIKHOV^{1,*}, A SALANOV¹, V SADYKOV^{1,2}, G GOLUBKOVA³ and O LOMOVSKII³

¹Boreskov Institute of Catalysis SB RAS, Novosibirsk, 630090, Russia

²Novosibirsk State University, Novosibirsk, 630090, Russia

³Institute of Solid-State Chemistry and Mechanochemistry SB RAS, Novosibirsk, 630066, Russia

MS received 1 June 2012; revised 26 October 2012

Abstract. Porous ceramic matrix composites $\text{FeAlO}_y/\text{FeAl}_x$ with incorporated metal inclusions (cermets) were synthesized by pressureless method, which includes hydrothermal treatment of mechanically alloyed FeAl powder followed by calcination. Their main structural, textural and mechanical features are described. Variation of FeAl powder alloying time results in non-monotonous changes of the porosity and mechanical strength. Details of the cermet microstructure and its relation to the mechanical properties are discussed.

Keywords. FeAl alloys; ceramic matrix composites; microstructure; texture; mechanical properties.

1. Introduction

Ceramometals (cermets) comprising of a ceramic matrix with uniformly distributed metallic particles have been studied for many years (Shelvin 1966; Kaplan and Avishai 2006). Porous cermets are promising catalysts for CH_4 dry reforming (Arkatova 2010) or partial oxidation into syngas (Tikhov *et al* 2006) as well as for Fischer–Tropsch synthesis (Tikhov *et al* 2007; Khodakov *et al* 2007).

Porous materials made from powdered FeAl alloys or their precursors are known to have high mechanical strength and stability at high temperatures. The methods traditionally used for preparation of porous FeAl-containing materials include high temperature treatment, which significantly decreases the volume of mesopores in the materials (Chen *et al* 2012). Recently, hydrothermal oxidation of aluminum powder producing porous $\text{Al}_2\text{O}_3/\text{Al}$ cermets was developed (Sadykov *et al* 2009) as a new pressureless approach to the synthesis of porous catalyst supports. The hydrothermal oxidation of a portion of an aluminum sample results in the formation of aluminum hydroxide. This way, particles of the powder become consolidated into a mechanically strong porous monolith by producing the hydroxide. Additional calcinations are essential to give higher mechanical strength and increase the mesopore volume as a result of hydroxide-to-oxide transformations (Sadykov *et al* 2009). However, these cermets suffer from the low melting temperature of aluminum.

The use of mechanically alloyed MeAl powders as the precursors is the next step in improving the cermet properties and achieving higher thermal stability. Mechanical alloying

is a powerful way to synthesize powdered alloys and intermetallics from individual metals. For instance, FeAl alloy powder can be easily synthesized using a planetary ball mill (Grigorieva *et al* 2001). Earlier mechanical alloying followed by hydrothermal treatment and calcination was successfully used to synthesize $\text{CrAlO}_y/\text{CrAl}_x$ cermets (Tikhov *et al* 2006). This study is devoted to the synthesis of a new material $\text{FeAlO}_y/\text{FeAl}_x$ by partial oxidation of FeAl (70:30) powders alloyed for different times and characterization of its main properties.

2. Experimental

Commercial grade aluminum (PAP-1, Russian grade GOST 5499-71) and iron (GOST 9849-86) powders were used as precursors. The preparation procedure of the porous cermets included the following steps. (a) A mixture of metal powders containing 70 at% iron and 30 at% aluminum was subjected to mechanical activation (MA) in a high-power planetary ball mill APF (the acceleration of the balls was 600 m/s^2 , balls:powder weight ratio was 200:10, the ball diameter, 5 mm and the milling time was varied in the range of 2–11 min), (b) the alloyed precursor was loaded into a stainless-steel die specially constructed to ensure free access of water and hydrogen release. The loaded die was placed into boiling water (hydrothermal treatment, HTT) and kept there for 4 h producing a strong monolith (diameter, 1 cm, length, 8 cm) and (c) finally, the granulated product was removed from the die, dried for 1 h at 120°C and calcined in air with gradual increase of temperature up to 900°C . The calcination yielded a mechanically strong material. In order to avoid explosion at the mechanical alloying stage, we used a special aluminum powder covered by organics

*Author for correspondence (tikhov@catalysis.ru)

(Tikhov *et al* 2005). The mill was specially cooled by water. The maximum amount of aluminum was also limited (~ 20 wt%).

The phase composition was characterized by XRD using URD-63 diffractometer with $\text{CuK}\alpha$ radiation in 2θ range of $20\text{--}70^\circ$. The average size (L) of iron crystallites was calculated using Scherrer's equation. The porosity was estimated from the values of true and apparent densities of the granulated cermets. The true densities of the samples were measured using a Micromeritics Autopycnometer 1320 helium pycnometer. Specific surface areas (SSA) were determined by low temperature (77 K) nitrogen adsorption on the Micromeritics ASAP-2400 instrument. In order to improve the accuracy, total amount of the sample was selected to ensure the total specific area not less than 10 m^2 . The packed density of the powdered MA product was measured from the mass and volume of the powder loaded into the glass cylinder after shaking for several minutes. The crushing strength of the pellets (diameter, ~ 10 mm and height, ~ 3 mm) was measured using a PK-2-1 instrument. This method is described in detail elsewhere (Ismagilov *et al* 1999) and is used very often in Russia for characterization of the mechanical properties of granulated supports and catalysts.

Details of the microstructure were studied using a scanning electron microscope JEOL JSM-6460LV equipped with an EDX-INCA/Energy-350 (Oxford Inst.) attachment for point analysis of the cermet components. The samples for SEM were sealed into epoxy and polished to obtain flat cross-sections. The accelerating voltage used for registration of SEM images and EDX analysis of surface segments was equal to 25 keV. The atomic concentrations obtained after the standard computer processing included decimal values. The approximate stoichiometry of the oxides was estimated assuming that aluminum oxide had $\text{AlO}_{1.5}$ stoichiometry. Thermal analysis was carried out using a Q-1500D instrument (Hungary) at 10 K/min heating rate in helium flow.

3. Results and discussion

3.1 Evolution of Fe–Al powdered precursors with MA time

Evolution of the phase composition of Fe–Al powders with MA time is presented in figure 1(a). The intensity of the peaks attributed to Al (JSPDS 04-0787) gradually decreased with MA time until they disappeared after 11 min. Meanwhile, some amorphous phases (marked with an arrow) appeared. Probably, this is a solid solution of Al in Fe–Fe(Al) as described in Enayati and Salehi (2005). The formation of an intermetallic phase such as Fe_2Al_5 (Yelsukov and Dorofeev 2004) is not observed, probably, due to fast MA processes occurring in APF-type mill in our experiments. For example, under our conditions, transformation of the layered microstructure to the uniform one occurred between 5 and 8 min of milling (figure 2a,b). Meanwhile, Enayati and Salehi (2005) observed the layered microstructure even after milling for several hours.

During MA, the average crystallite size (CSR) of Fe (figure 3) decreased monotonously from ~ 80 to ~ 45 nm. The same tendencies were observed for different types of MeAl powders (Pabi *et al* 1997). The average particle size also decreased, leading to an increase of the loading (packed) density of the powders in the die with MA time (figure 3). So, the main characteristics of Fe–Al powders, except for the microstructure, changed monotonously with MA time.

3.2 Evolution of cermet structure during MA of initial powder

First of all, variation of Fe–Al powder composition leads to changes of the reactivity at the following stages of cermet formation (hydrothermal treatment and calcination). According to the thermal analysis data in the air flow (not presented for brevity), the relative weight gain of FeAl alloys after MA and HTT under high temperature oxidizing treatment decreased from 28 to 17 wt%, when the alloying time of the powdered precursors was increased. So, the increase of MA time at first stage of synthesis makes the metal component more resistant to oxidation at high temperatures at the second stage.

However, oxidation is not the only process taking place during calcination. This is illustrated by the thermal analysis data in He flow (figure 4). A large exothermic peak observed at $410\text{--}380^\circ\text{C}$ shifted to lower temperature and disappeared after 11 min MA. According to XRD (figure 1a), this peak disappears only after the disappearance of the peak attributed to aluminum metal in the powdered precursor (figure 1a). The same phenomenon was observed earlier (Enayati and Salehi 2005). Undoubtedly, this effect is related to some rearrangement in the metal. Earlier, it was attributed to the process $\text{Fe}(\text{Al}) \rightarrow \text{Fe}_3\text{Al}(\text{FeAl})$ (Enayati and Salehi 2005).

According to XRD data (figure 1b), the cermets consist of ceramic and metal components. The main oxide phases are corundum (JSPDS 46-1212) and hematite (JSPDS 33-0664). Maghemite (JSPDS 39-1346), magnetite (JSPDS 19-0629) and spinel FeAl_2O_4 (JSPDS 34-0192) are minor phases. The metal components are *bcc* iron (JSPDS 06-0696) and iron–aluminum intermetallic FeAl (JSPDS 45-0983) formed, probably from an amorphous phase, such as Fe(Al) solid solution (Enayati and Salehi 2005). The measurements of the relative intensities of the metal and ceramic components clearly show that the metal content in cermets increases when longer alloying times are used (figure 1b). This is consistent with the thermal analysis data.

Polished surfaces of the cermets showing their microstructure are presented in SEM micrographs (figures 2(c,d) and 5). A lot of macropores up to several μm in size are observed in all the samples. A qualitative comparison of the cermets prepared using 2 min MA (figure 5a) and 11 min MA (figure 5d) shows that the number of macropores significantly decreases when the alloying time gets longer. According to EDX spectra, the porous matrix consists

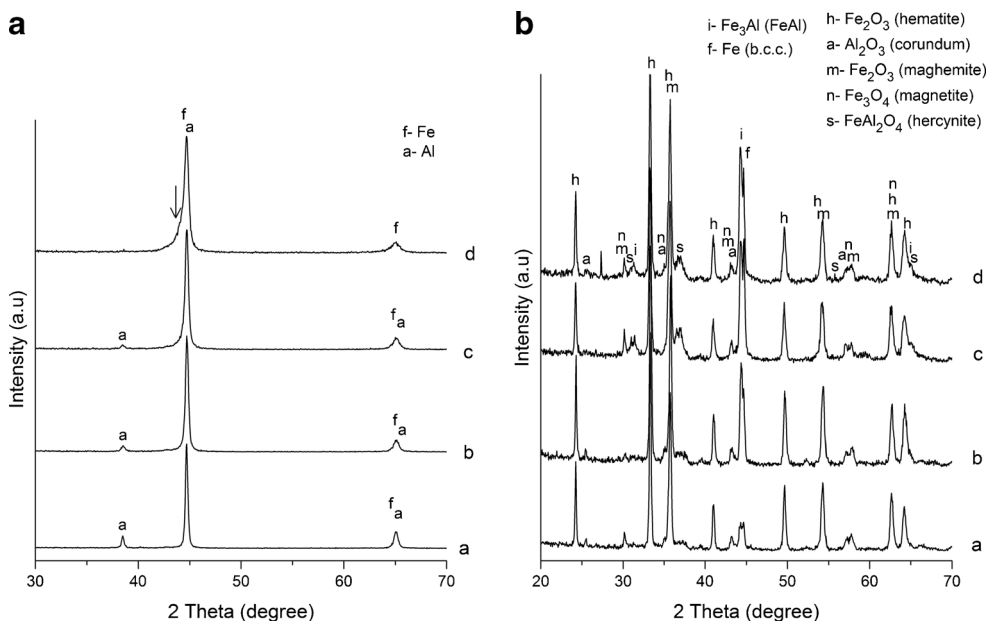


Figure 1. (a) XRD patterns of FeAl powders with different times of preliminary mechanochemical activation τ_{MA} (min): a, 2; b, 5; c, 8 and d, -11 and (b) XRD patterns of $\text{FeAlO}_y/\text{FeAl}_x$ made from FeAl powders with different times of preliminary mechanochemical activation τ_{MA} (min): a, 2; b, 5; c, 8 and d, -11.

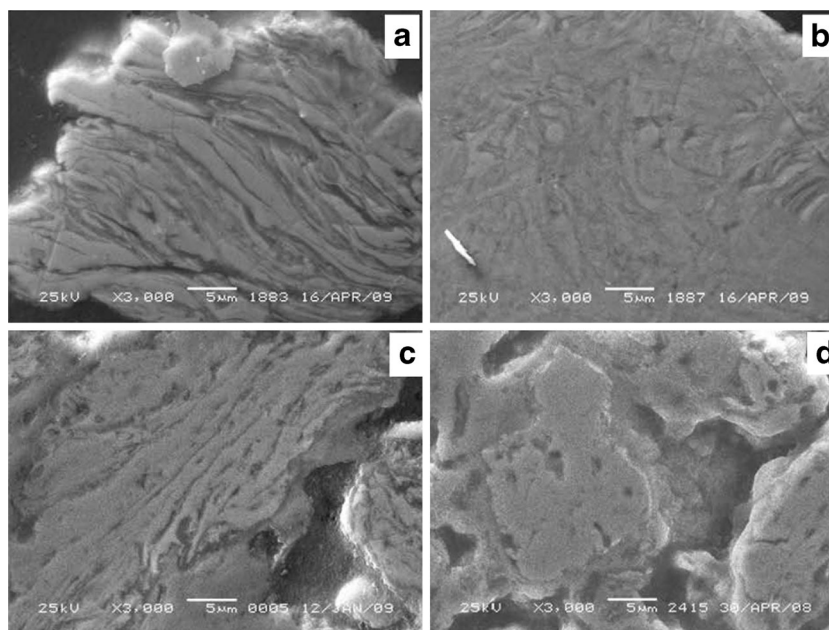


Figure 2. SEM micrographs of cores in FeAl powders (a,b) and $\text{FeAlO}_y/\text{FeAl}_x$ cermets (c,d) prepared from FeAl powder with different MA times (min): a,c, -5 and b,d, -8.

of iron, aluminum and a substantial amount of oxygen (figure 5(a-d), point 1). So, aluminum (III) and iron (III) oxides are the main phases forming the matrix.

In addition, dense inclusions are randomly distributed in the porous matrix. Their microstructure and composition strongly depend on the alloying time of the precursor alloy.

Layered inclusions are dominant at short alloying times (figure 2c). The oxidizing conditions lead to oxygen incorporation in these inclusions in significant concentrations up to 10–45 mol%. However, oxygen content in the inclusions is much lower than the oxide matrix. Probable compositions of the inclusions are presented in figure 5.

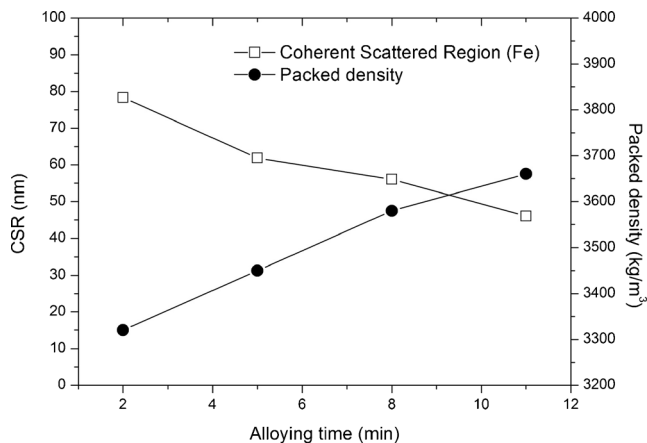


Figure 3. Dependence of powder packed density and Fe grain size (CSR) in FeAl powders on time of preliminary mechanochemical activation.

The increase of the alloying time leads to disappearance of the layered structure and formation of uniform irregularly shaped inclusions with closed pores in the cermets (figure 2d). The oxygen concentration in these inclusions is low. So, the main phases are metals with Fe/Al ratio of about 3–4. Composition of inclusions is close to that of the intermetallic phases Fe_3Al or $\text{FeAl} + \text{Fe}$, which agree well with the diffraction data. Hence, formation of uniform microstructure with MA time promotes stability of Fe–Al alloys to bulk oxidation.

3.3 Factors determining porosity and crushing strength of cermets

Figure 6 shows that variation of the crushing strength is not monotonous. It should have been mentioned that the data about compressive strength are rather rough but their precision is sufficient to make this conclusion. The maximum of the crushing strength (sample with 8 min alloying time) corresponds to the minimum of the cermet porosity (figure 6). Porosity first decreases from 25 to 11%, then increases to 15%. The relation between porosity and crushing strength is common for the majority of porous bodies described in Tikhov *et al* (2004) and Sadykov *et al* (2009). So, the mechanical properties of cermets are also related to their porosity. However, the factors determining the non-monotonous porosity variation are very different.

First of all, the total pore volume of porous cermets consists of different types of pores. These include mesopores determined by adsorption methods (lesser than 50 nm), macropores (0.1–1 μm) and ultramacropores (1–100 μm). Ultramacropores are formed by voids between particles of the powdered MA product (Sadykov *et al* 2009). So, they should be related to the loading density of the powdered MA product. This density monotonously decreases with MA time (figure 3). Qualitatively, this is in agreement with SEM data for cermets (figure 5) showing that the number and size

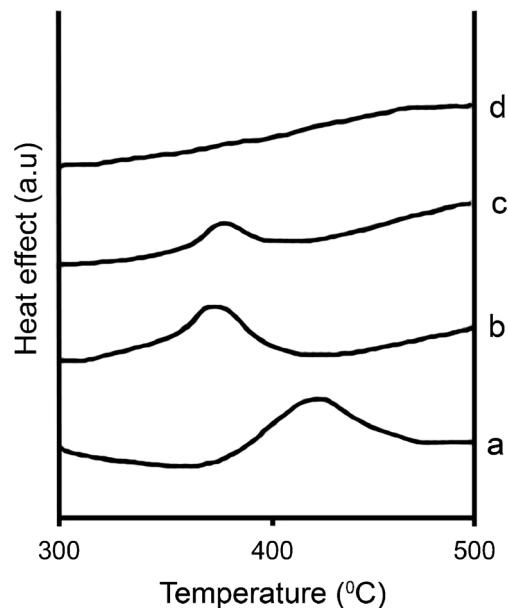


Figure 4. Thermal analysis data of Fe–Al precursors after MA and hydrothermal treatment in He flow. MA times: a, 2 min, b, 5 min, c, 8 min and d, 11 min.

of ultramacropores decreases with MA time. So, the ultramacroporosity is not related to the non-monotonous crushing strength.

The mesopore structure is related to the specific surface area (Fenelonov 1994). The dependence of the cermet specific surface areas on the crushing strength also has a minimum (figure 6). Earlier, the specific surface area of cermets prepared from powders containing aluminum was related by us to the oxide matrix formed after the hydrothermal treatment and calcination (Tikhov *et al* 2004; Sadykov *et al* 2009). But the concentration of the oxide matrix in $\text{FeAlO}_y/\text{FeAl}_x$ composites decreases monotonously with MA time of Fe–Al blend precursor. We demonstrated this fact using XRD and thermal analyses. Also SSA is very low compared to other porous cermets (Sadykov *et al* 2009). So, we concluded that SSA of $\text{FeAlO}_y/\text{FeAl}_x$ cermets is determined to a large extent by SSA of the metal inclusions.

The microstructure of the cermet inclusions also significantly depends on the alloying time of Fe–Al blend. As mentioned above, the cermet sample with 8 min MA demonstrated a substantial change. The layered structure was replaced by a uniform structure with inner porosity of the metal inclusions (figure 2d). Probably, the transformation of Fe–Al microstructure from layered to uniform leads to a significant decrease of the cermet open porosity as well as specific surface area (figure 6) due to blocking of open mesopores by the cermet metal inclusions at high temperature. Calcination of the cermet precursor made from the powdered product with 3 and 5 min MA with aluminum in the layered microstructure results in its oxidation in agreement with EDX data. This leads to the formation of open pores. A substantial change of the powdered precursor microstructure at

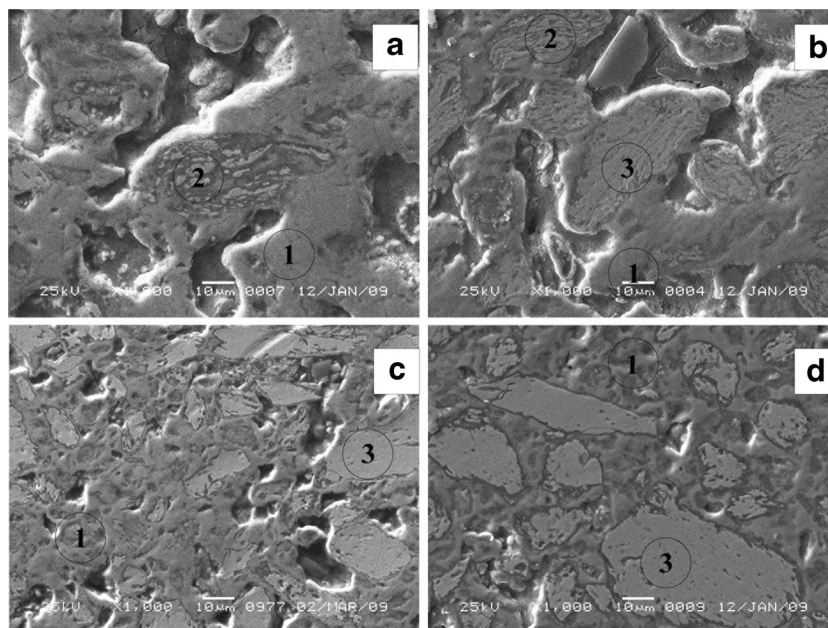


Figure 5. SEM micrographs of FeAlO_y/FeAl_x cermets prepared from FeAl powder after different MA times (min): a, 2; b, 5; c, 8 and d, -11. Different points were used for EDX analysis: (i) – (Fe₂O₃+ Al₂O₃); (ii) (Al₂O₃+Fe₃O₄+Fe⁰) or (Fe₃O₄+FeAl) and (iii) (Fe₃Al or FeAl + Fe⁰).

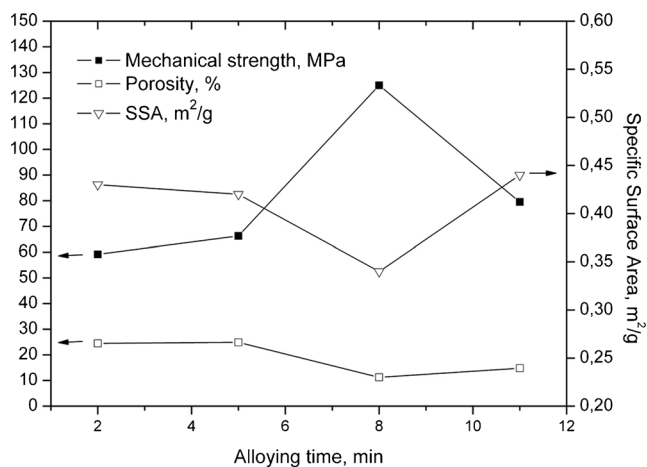
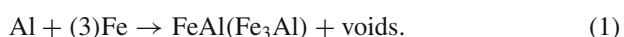


Figure 6. Dependence of specific surface area (i), porosity (ii) and crushing strength (iii) of FeAlO_y/FeAl_x cermets at time of preliminary mechano-chemical activation.

8 min MA is accompanied by the preservation of some aluminum grains in the bulk of powder particles (figure 1(a)). These aluminum grains in the bulk of the particles can form voids in the metal inclusions of cermets after calcination at high temperatures due to formation of denser intermetallics (true density of about 6.7 (Trojanskii *et al* 2004)) from aluminum (true density, 2.7) and iron (true density, about 7.9) according to the process:



At longer MA (11 min) of FeAl powder, pure aluminum grains are absent in the bulk of the powder particles with uniform distribution due to alloying with iron. Formation of closed pores in the metal inclusions decreases the true density from 5.1 g/ml for 5 min MA alloyed cermet to 4.9 g/ml for 8 min MA one. The disappearance of Al metal in 11 min MA powder leads to the increase of cermet density to 5.1 g/ml. Another possible source of the voids is the supersaturated solid solution (SSS) described in Yelsukov and Dorofeev (2004) and Enayati and Salehi (2005). These solid solutions have low true densities of about 3.8 g/ml (Mondolfo 1976). However, SSS concentration should gradually increase with MA time and should not correlate with the porosity or the crushing strength. So, variation of the microstructure at MA stage leads to the variation of porosity of the metal inclusions as well as the mechanical properties of Fe–Al cermets.

3.4 Comparison to other porous materials

The mechanical properties and pore structure are of great importance for heterogeneous catalysts and supports (Fenelonov 1994). FeAlO_y/FeAl_x composites have lower crushing strength than non-porous construction ceramics (Kaplan and Avishai 2006) or metallic foams (Leonov *et al* 1998). Still, the FeAlO_y/FeAl_x cermets have much better mechanical properties compared to conventional porous ceramics (Ismagilov *et al* 1991), Al₂O₃/Al cermets (Tikhov *et al* 2004) or even CrAlO_x/CrAl composites

(Tikhov 2006). This makes them promising materials for specific catalytic processes demanding high attrition resistance. The porosity of $\text{FeAlO}_y/\text{FeAl}_x$ composites is not very high (figure 6). It can be increased by adding mesopore materials to the cermet precursor. Another way to develop the macropore structure is blending of MA product with powdered flammable materials, which disappear after calcination. This search will become the goal of our future work.

Ceramometals can be shaped as rings, honeycombs as well as thick coating on metallic tubes (see Tikhov et al 2005; Sadykov et al 2009) depending on the design of a stainless-steel die.

4. Conclusions

Porous ceramic–matrix composites $\text{FeAlO}_y/\text{FeAl}_x$ were synthesized by hydrothermal oxidation of mechanically alloyed FeAl powder followed by high temperature calcination. The structural, textural and mechanical properties of cermets were investigated. The mechanical alloying of the powdered precursor was found to affect main properties of cermets. This mechanical alloying leads to variation of the powdered precursor microstructure from the layered to the uniform one. As a result, resistance to oxidation treatment is gradually increased. The textural and mechanical properties of the cermets were varied non-monotonously. The crushing strength of $\text{FeAlO}_y/\text{FeAl}_x$ cermets reaching 125 MPa was found to be related to the microstructure of the metal inclusions and porosity of the cermets.

Acknowledgments

This work was supported by RFBR Grant No. 11-08-00704.

References

- Arkatova L A 2010 *Catal. Today* **157** 170
- Chen G, Cao P, He Yu, Shen P and Gao H 2012 *J. Mater. Sci.* **47** 1244
- Enayati M H and Salehi M 2005 *J. Mater. Sci.* **40** 3933
- Fenelonov V B 1994 *React. Kinet. Catal. Lett.* **52** 367
- Grigorieva T F, Barinova A P and Lyakhov N Z 2001 *Rus. Chem. Rev.* **70** 52
- Ismagilov Z R, Shepeleva M N, Shkrabina R A and Fenelonov V B 1991 *Appl. Catal.* **69** 65
- Ismagilov Z R, Shkrabina R A and Koryabkina N A 1999 *Catal. Today* **47** 51
- Kaplan W D and Avishai A 2006 *Ceramic matrix composites (Microstructure, properties and applications)* (ed.) I M Low (Cambridge, England: Woodhead Pub. Ltd.) p. 285
- Khodakov A Y, Chu W and Fongarland P 2007 *Chem. Rev.* **107** 1692
- Leonov A N, Smorygo O L, Romashko A N, Dechko M M, Ketov A A, Novikov L A and Tankovich V S 1998 *Kinet. Catal.* **39** 634
- Mondolfo L F 1976 *Aluminum Alloys: Structure and Properties* (London-Boston: Butterworth & Co Ltd) p. 246
- Pabi S K, Joardar J, Manna I and Murty B S 1997 *Nanostruct. Mater.* **9** 149
- Sadykov V A, Parmon V N and Tikhov S F 2009 *Compos. Interf.* **16** 457
- Shelvin S S 1966 *Cermets*. (eds) J R Tinkelpaugh and W B Grandall (New York: Reinold Publ. Corp.) p. 153
- Tikhov S F, Potapova Yu V, Fenelonov V B, Sadykov V A, Salanov A N, Tsybulya S V and Melgunova L F 2004 *Kinet. Catal.* **45** 642
- Tikhov S F, Romanenkov V E, Sadykov V A, Parmon V N and Ratko A I 2005 *Kinet. Catal.* **46** 682
- Tikhov S F et al 2006 *Stud. Surf. Sci. Catal.* **161** 641
- Tikhov S F et al 2007 *Stud. Surf. Sci. Catal.* **163** 153
- Troyanskii A A, Ryabtsev N N and Galyan N N 2004 *Mod. Electrometallurgy* **3** 11 (in Russian)
- Yelsukov E P and Dorofeev G A 2004 *J. Mater. Sci.* **39** 5071